

---

This is the **accepted version** of the article:

Folberth, Christian; Khabarov, Nikolay; Balkovic, Juraj; [et al.]. «The global cropland-sparing potential of high-yield farming». Nature sustainability, Vol. 3, Issue 4 (April 2020), p. 281–289. DOI 10.1038/s41893-020-0505-x

---

This version is available at <https://ddd.uab.cat/record/224224>

under the terms of the  **IN**  
COPYRIGHT license

# The global cropland sparing potential of high-yield farming

Christian Folberth, Nikolay Khabarov, Juraj Balkovič, Rastislav Skalský, Piero Visconti, Philippe Ciais, Ivan A. Janssens, Josep Peñuelas, Michael Obersteiner

## Summary

The global expansion of cropland exerts substantial pressure on natural ecosystems and is expected to continue with population growth and affluent demand. Yet, earlier studies indicated that crop production could be more than doubled if attainable crop yields were achieved on present cropland. Here we show based on crop modelling that closing current yield gaps by spatially optimizing fertilizer inputs and allocation of 16 major crops across global cropland would allow to reduce the cropland area required to maintain present production volumes by nearly 50% of its current extent. Enforcing a scenario abandoning cropland in biodiversity hotspots and uniformly releasing 20% of cropland area for other landscape elements, still enabled reducing the cropland requirement by almost 40%. As a co-benefit, greenhouse gas emissions from fertilizer and paddy rice, as well as irrigation water requirements are likely to decrease with reduced area of cultivated land, while global fertilizer input requirements remain unchanged. Spared cropland would provide space for substantial carbon sequestration in restored natural vegetation. Only targeted sparing of biodiversity hotspots supports species with small-range habitats, while biodiversity would hardly profit from a maximum land sparing approach.

## Introduction

Globally, agricultural activity and the continuous expansion of croplands impose wide-ranging environmental burdens on natural ecosystems. Intensively managed cropland is characterized by excessive and imbalanced applications of N and P, whereas low-input agricultural systems result in nutrient-poor soils and low yields<sup>1,2</sup>. Globally, freshwater use in agricultural irrigation consumes about 70% of total water withdrawals<sup>3</sup>, and cropland farming contributes about 5% of global GHG emissions, mainly through emissions of paddy rice methane (CH<sub>4</sub>) and soil nitrous oxide (N<sub>2</sub>O) from added mineral N fertilizer and manure<sup>4</sup>. Biodiversity loss is challenging to quantify, but estimated to exceed safe boundaries, primarily due to habitat loss<sup>5</sup>. Most recently, the land sparing debate<sup>6–9</sup> has gained new momentum from the Half Earth project<sup>10</sup> that aims to return half the area of land under anthropogenic management to natural land cover to restrict biodiversity losses and abate other externalities of anthropogenic land use<sup>6</sup>. The need for this type of strategy is even more urgent, given the increasing global demand for agricultural products<sup>11,12</sup>. Yet, biophysical benchmarks for ambitious land sparing targets and associated externalities remain virtually unknown.

Earlier studies have suggested that cropland will likely further expand in the future due to population growth and climate change<sup>13</sup>, while effective cropland sparing would need to involve measures such as dietary change to reduce crop demand<sup>14–16</sup>. In contrast, global nutrient input intensification, crop switching, and expansion of irrigated land may increase global crop production volumes by up to 150% for major crops<sup>17–21</sup> depending on whether and how these strategies are combined. Intensification has also been identified in conceptual and semi-quantitative studies as a promising strategy for the abatement of land conversion, expansion of natural land cover<sup>7,8,22</sup>, and reduction of environmental impacts, depending on management specifics<sup>23</sup>. However, while average yields for major crops have

been increasing globally during the past decades, they have stagnated or decreased in various parts of the world and the present pace in yield gains is considered insufficient to meet future crop demand<sup>24</sup>. Persisting global yield gaps in major crops have been attributed foremost to nutrient deficits and to a lesser extent to insufficient water supply<sup>19</sup>.

## **Estimating global cropland requirement**

In this study, we quantified the potential of land sparing through intensification of nutrient inputs to meet plant requirements and optimal spatial allocation of 16 major crops to estimate a lower boundary of cropland requirement for meeting present crop demands (Figure 1). We used the established global gridded crop model EPIC-IIASA<sup>17</sup> to estimate non-nutrient limited crop yields, with and without sufficient irrigation water supply, depending on land use information to avoid expansion of irrigated land. EPIC-IIASA combines the process-based agronomic model Environmental Policy Integrated Climate<sup>25,26</sup> (EPIC) with a global data infrastructure gridded at 5' x 5' resolution. The 5 arcmin grid cells with identical soil texture and topography classes and located within the same 30' x 30' climate grid and administrative region were aggregated to simulations units. The resulting 120000 simulation units thus vary in size from 5' x 5' to 30' x 30' or total corresponding surface areas from 69 to 2500 km<sup>2</sup> near the equator depending on input data heterogeneity (Supplementary Figure S19; Supplementary Text S2). Maps of present cropland were aggregated from 5' x 5' source data to the same spatial scale of simulation units to provide consistent input data on area and crop yields for the cropland allocation model.

Crop distributions were spatially allocated using a linear optimization algorithm under three simple criteria that comprised minimizing the extent of current global cropland; maintaining 2011-2015 global production volumes for each crop; and avoiding novel expansion of cropland locally. This was done (I) allowing the full use of the current cropland in each simulation unit to create a global “maximum land sparing” (MLS) scenario or (II) with a complete release of annual cropland in biodiversity hotspots and a forced release of at least 20% of cropland area in each simulation unit to create a “targeted land sparing” (TLS) scenario. The first serves for providing a benchmark of what extent of land sparing is technically feasible given present agricultural technologies. The latter provides a benchmark for a global scenario focused on habitat restoration for threatened species in hotspots combined with the establishment of uniformly distributed landscape compartments as wildlife habitats<sup>27</sup> or buffers for adverse impacts of high-input agriculture<sup>28</sup>. Two supplementary scenarios serve for assessing how constraining crop distributions to their present growing regions (scenario MLS<sub>ncs</sub>) or allowing crops to cover a maximum of 34% cropland in a simulation unit – indirectly increasing crop diversity locally - (scenario MLS<sub>wcd</sub>) affect results in the MLS scenario. As such, these scenarios are hypothetical, leaving aside policy- and socio-economic implications, but they can nonetheless inform decision-makers about the bio-physical feasibility of ambitious land sparing targets. While the focus of our analysis is on cropland sparing potential, we also quantified, based on model results directly or auxiliary datasets, changes in requirements for N and P fertilizer and irrigation water; selected GHG emissions; carbon (C) storage in resultant, expanded areas of natural vegetation; and potential increase in natural habitats for wildlife. Further details are provided in the Methods section.

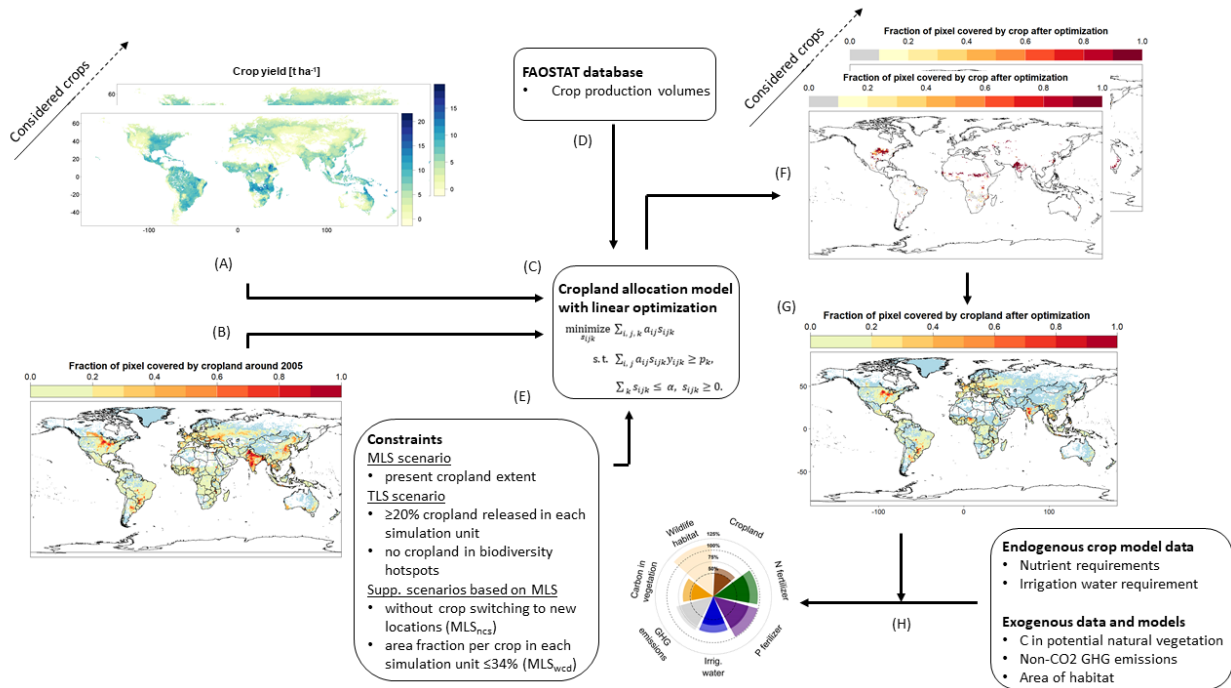


Figure 1: Schematic of the study design. Attainable crop yields (A) from the EPIC-IIASA global gridded crop model (or statistically derived yield datasets) are combined with present cropland data for these crops (B) from SPAM2005 (or other suitable land use datasets) into a linear optimization model (C). This model has the objective to minimize cropland extent via cropland allocation based on land use efficiency while maintaining present production volumes (D) for two main scenarios (I) with the only constraint of presently available cropland (MLS scenario) or (II) with imposing a release of cropland in biodiversity hotspots and a uniform global release of 20% cropland (TLS scenario). Further constraints (E) are introduced for two supplementary scenarios (see Methods). The optimization results in crop-specific land use datasets (F), which are aggregated to total remaining cropland including the crops not considered in the optimization (G). Externalities (H) are quantified based on outputs of the crop model itself (nutrient input and irrigation water requirement) or based on external data and models (carbon sequestration potential, change in area of habitat, and greenhouse gas emissions). Crop model simulations and cropland allocation were performed at the level of globally 120000 simulation units aggregated from 5' x 5' pixels (about 8.3 km x 8.3 km near the equator) to a maximum size of 30' x 30' (about 50 km x 50 km near the equator) based on physical heterogeneity and administrative borders. The cropland area in each 5' x 5' pixel was subsequently scaled according to the relative change in cropland extent in the overlying simulation unit (see Supplementary Figure S19) for the estimation of externalities and visualization. The central cropland allocation scheme is shown for exemplary simulation units in Supplementary Figure S18.

## Global cropland sparing potential and spatial patterns

Intensification and optimal crop reallocation under the MLS scenario decreased the cropland requirement to nearly 50% of the baseline for all crops and to 46% for the 16 selected crops (Figure 2). The greatest sparing potential was for typical smallholder crops, such as sorghum and pulses, with >80% of land released (Supplementary Table S1). Lower land gains (<50%) were estimated on the other hand for crops for which production tends to be highly intensified, such as maize, rice, soybean, wheat, and sugar crops. The TLS scenario also reduced cropland area to remaining 62% of the baseline, indicating that radical reductions in cropland area are not restricted to a narrow set of solutions, and high yields may be sustained across large regions for most crops. Results were highly comparable for a wider range of land use and attainable crop yield datasets, showing that our estimates are robust within the limits of available data (Supplementary Text S1 and S2).

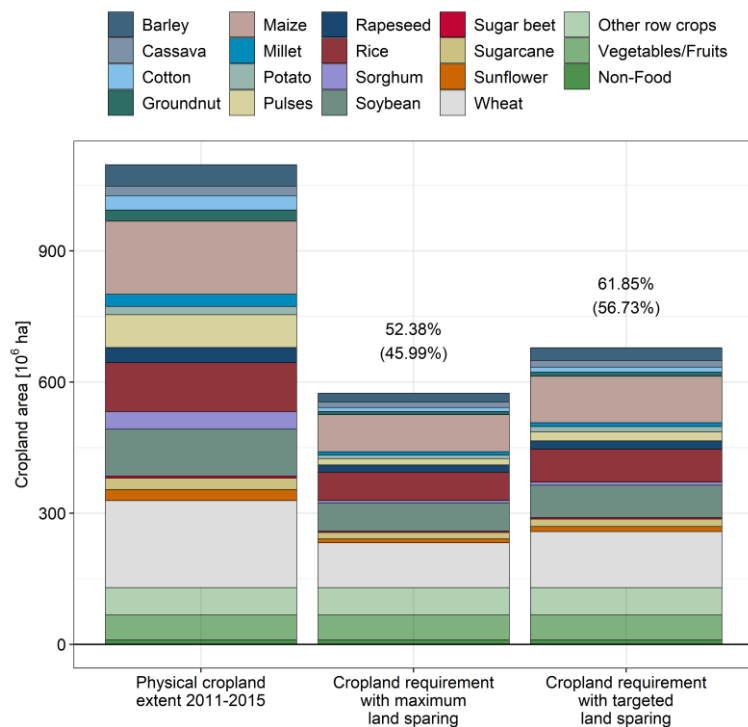


Figure 2: Global extent of annual cropland in the reference period 2011-2015 (column one), and estimated area of cropland of 16 major crops optimized for maximum sparing potential (column two) and sparing of at least 20% of cropland in each simulation unit and completely abandoning biodiversity hotspots (column three). Crops not considered in the optimization are aggregated into three groups at the base of each bar. Percent values refer to area of total annual cropland (upper) and simulated crops (lower, in parentheses). Globally, annual crops plus sugarcane extended to about 1100 Mha of cropland during the reference period<sup>29</sup>, of which about 950 Mha were planted with the crops considered in the optimization (major cereals, grains, pulses, and sugar). The remaining 150 Mha encompassed “Other row crops”, “Fruits and Vegetables”, and “Non-food/feed crops” shown at the base of each bar (Supplementary Table S1).

Contiguous regions of cropland release in the MLS scenario are primarily located in agro-climatically unfavourable regions, such as the Western USA, Central Asia, and Sahel, but also in productive regions such as large parts of South Asia and in southern Russia (Figure 3b). Despite local concentrations of cropland in most productive areas, patterns of total fresh matter production volumes per continent remained comparable to the baseline with substantial and moderate gains in Africa and Asia at the cost of Europe and especially America (Supplementary Figure S4). The TLS scenario resulted in a wider distribution of cropland (Figure 3c), which is mostly driven by implicit cropland release in this scenario (Supplementary Figure S5). About 20% global annual cropland were released in biodiversity hotspots and globally uniform a minimum of 20% in the remainder of the cropland area (corresponding to 17% of global annual cropland). This left only a minor fraction of areas released subject to land use efficiency gains. These were again mostly located in agro-climatically adverse regions such as desert borders.

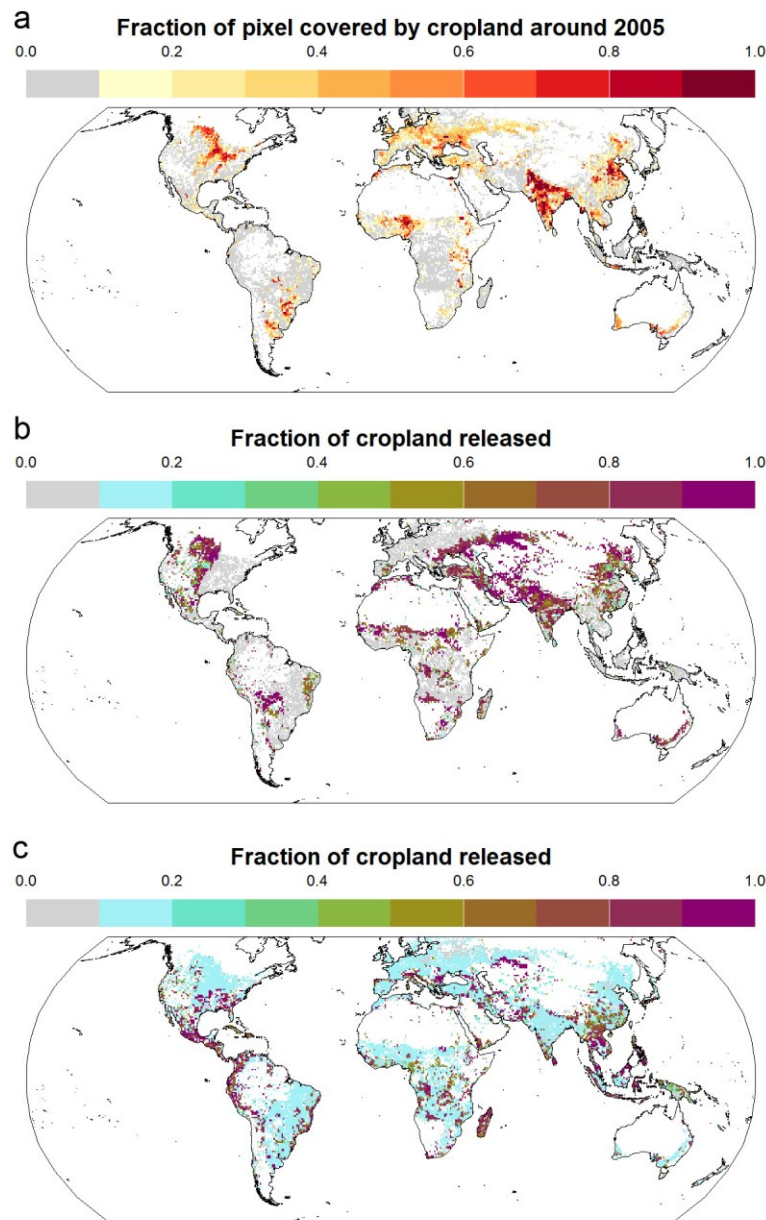


Figure 3: Proportion of each 5' x 5' pixel covered by cropland cultivated c. 2005 (SPAM dataset) (a) and fraction released after optimization of cropland requirement for maximum land sparing (b) and targeted land sparing with complete release of cropland in biodiversity hotspots and uniformly  $\geq 20\%$  of cropland (see Supplementary Figure S16) (c). Data in (b) and (c) correspond to bars two and three in Figure 2.

## Drawbacks of and barriers to cropland sparing and concentration

The release of cropland over large contiguous regions in both scenarios may entail substantial socio-economic implications with respect to livelihoods, as shown also in recent research on global conservation targets<sup>30</sup>, and may affect regional food self-sufficiency. Yet, the fact that patterns of cropland release are largely contrasting among the two scenarios indicates that a mixed approach, including the sparing of cropland in biodiversity hotspots only to the degree necessary for maintaining

wildlife habitats, could be implemented to balance socio-economic trade-offs with land sparing benefits among regions. Comprehensive global research on social acceptance for land sparing is lacking and certainly context-dependent. Conceptual studies suggest a range of policy measures from financial compensation for abandoned cropland to payments for restored vegetation management and further knowledge transfer and infrastructure for improved crop management to steer policy implementations of intensification for cropland sparing<sup>8</sup>. Notwithstanding, the reconciliation of global targets with local and regional stakeholder demands will require holistic approaches bridging these scales, which likely poses the greatest challenge in achieving effective global land sparing<sup>31,32</sup>. And any further concentration of crop production will increase the already extensive reliance of large parts of the world on food imports, amplifying the requirement for resilient global trade systems<sup>33</sup>.

Spatial shifts in crop cultivation areas are a constant process<sup>34</sup> and have been subject to disruptive regime shifts for specific crops and regions in the past<sup>35</sup>. Both do not necessarily follow patterns of domestic demand but serve often for income generation and diversification<sup>36</sup>. However, the adoption of new crops or farming practices in general requires more information and policy interventions in regions in which they are not practiced so far. Analysing the spatial occurrence of crops in both scenarios herein reveals that <20% of resulting cropland area are occupied by crops in simulation units in which they are presently not grown, and <1% in major Koeppen-Geiger climate regions and countries in which the respective crops are presently not cultivated (not shown). Constraining the cropland allocation model to only assign crops in the MLS scenario to simulation units in which they are presently cultivated while allowing their local acreage to change (supplementary scenario MLS<sub>ncs</sub>) results in 1% lower land sparing potential (Supplementary Figure S6). This indicates that the free shifting of crops is not a key mechanism behind our findings and that crops are already cultivated in regions in which they are or can be most productive. Yet, areas of crops presently cultivated for cultural and historic reasons may be given up in the model. In this context, it needs to be stressed that our study aims to provide information on the cropland that is essentially required to meet present demand and should not suggest to abandon agriculture in places in which it provides important local cultural and social services.

Furthermore, optimizing cropland distribution based on land use efficiency may result in wide-spread monocropping systems with higher vulnerability to biotic and abiotic stressors, high requirement for pest control agents, and little provision of on-farm biodiversity. To address the impact of enforcing crop diversity on cropland sparing potential, we evaluated a supplementary scenario allowing only up to 34% of each simulation unit to be covered by a specific crop in the MLS scenario (supplementary scenario MLS<sub>wcd</sub>). This reduces the cropland sparing potential by 5% relative to the present extent (Supplementary Figure S6) while resulting in the co-occurrence of 2-3 crops in most simulation units (Supplementary Figure S8). The concurrence of several crops translates into the feasibility of inter-annual crop rotations, which are a key measure for integrated crop protection<sup>37</sup>. Due to the capped area share of single crops, simulation units with only one or two crops attributed can similarly implement rotating inter-annual fallows. This supplementary scenario also results in higher crop diversity at the continental scale, especially in Europe, compared to the other land sparing scenarios (c.f. Supplementary Figure S7 and Supplementary Figure S4).

## **Associated changes in externalities**

Reductions in cropland area, combined with optimal N and P fertilization, may reduce or at least not exacerbate major agricultural input requirements and externalities globally (Figure 4). We found that

total N and P application would increase by only 6% in the MLS scenario, and decrease by 1-4% in the TLS scenario. This includes the presently inevitable prevalence of substantial nutrient losses such as leaching and erosion. Our results confirm that current excessive and imbalanced nutrient supply outweigh soil nutrient mining<sup>2</sup> and that the reduction in area of nutrient-mined soils, which can be expected to increase the exogenous nutrient demands for closing yield gaps in our scenarios, can be compensated by reduced applications of N and P tailored to meet crop demands in areas of presently excessive fertilization (Supplementary Text S3). Yet, locally, foremost N and partly P surpluses may well exceed those reported for around the year 2000, depending on which input sources are considered (Supplementary Figure S11). Especially the MLS scenario results in a shift towards higher local N surpluses per area whereas the TLS scenario closely resembles past patterns of conservative estimates neglecting inputs from manure, deposition, and biological fixation. For the TLS scenario, low P surpluses occur more frequently, in part due to the larger extent of remaining cropland compared to the MLS scenario, which again exhibits a more frequent occurrence of moderate to high surpluses. Notably, the latter is also caused by a larger fraction of cropland remaining in tropic regions in which weathered soils with high P fixation occur more frequently<sup>38</sup>.

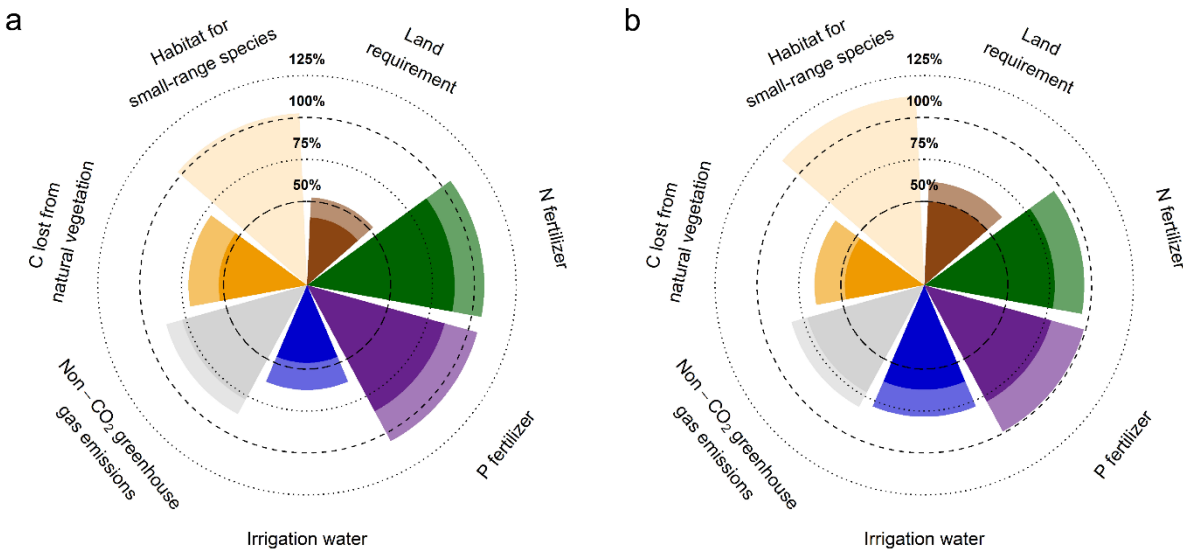


Figure 4: Changes in key agricultural externalities following optimization of area of cropland for (a) maximum land sparing (bar 2 in Figure 2) or (b) targeted land sparing (bar 3 in Figure 2), compared with the baseline scenario (100% circle; see bar 1 in Figure 2; status in 2011-2015) for 16 major crops (dark colors) and the remaining annual crops (light colors; not estimated for biodiversity potential). Proportions of nitrogen (N) and phosphorus (P) fertilizer, and irrigation water applied to crops during the reference period were extrapolated linearly from crops in c. 2000 reported by Mueller et al.<sup>19</sup>, or for irrigation water from Siebert and Doell<sup>3</sup>. Greenhouse gas emissions comprise methane from rice and nitrous oxide from fertilizer and assume the other major sources (manure and crop residue) remain unchanged. Carbon (C) lost from potential natural vegetation is the amount of C stored in potential natural vegetation after cropland sparing relative to that during the baseline (100% of C in natural vegetation lost in cropland), using data from West et al.<sup>39</sup>. Habitat for small-range species is the average change in habitat area for terrestrial mammals intolerant to cropland in the lower quartile of range size distributions of terrestrial mammals in the IUCN Red List of Threatened Species<sup>40</sup> after recovery of natural vegetation on abandoned cropland. Details on the quantification of each externality are provided in the Methods.

Crop water requirement from irrigation decreased under the MLS scenario by 380 km<sup>3</sup> to 65% of the baseline (approx. 1100 km<sup>3</sup>), and under the TLS scenario by 218 km<sup>3</sup> to 78% of the baseline, precluding



losses within the irrigation system that exceed the actual global crop water requirement<sup>41</sup>. Water requirements vary with crop<sup>3</sup>, climate, and land surface extent<sup>42</sup>; hence the reduction in cropland area is a main driver of reduced irrigation volume. Thus, cropland sparing does not necessarily entail expansion of irrigation infrastructures if yields in rainfed regions are maximized by optimal fertilization and crop choice. This is consistent with earlier global and regional studies finding nutrient limitations to be a substantially more important driver for current yield gaps than irrigation<sup>19,43</sup>.

Greenhouse gas emissions from paddy rice and fertilized soils decreased to 87% and 82% (-0.15 and -0.21 Pg CO<sub>2</sub> equiv.) of the baseline in the MLS and TLS scenario, respectively. As N application remains fairly constant, this is mostly due to the decrease of CH<sub>4</sub> emissions from the reduced cultivation area for rice. Carbon (C) lost from potential natural vegetation is used as a proxy for C sequestration potential, if natural vegetation on spared cropland fully recovers. The largest C storage capacity occurs in tropical ecosystems, the lowest in arid climates<sup>39</sup>. Accordingly, the proportion of cropland remaining in the tropics under the MLS scenario (Figure 3b) resulted with 29% avoided loss of C from natural vegetation on present cropland in a proportionally low sequestration potential. However, this sequestration potential is equivalent to 20.5 Pg C, underpinning that land sparing for vegetation restoration may halt further deforestation that is a major contributor to global CO<sub>2</sub> emissions. The amount of C sequestration potential is higher in the TLS scenario, as major biodiversity hotspots are located in the tropics (Supplementary Figure S16). This increases the C sequestration potential to 24.2 Pg C.

The habitat suited mammal species with restricted ranges and intolerant to cropland (n=716) in presently cultivated regions increases substantially in the TLS scenario (+12.8%) but only marginally in the MLS scenario (+2.6%). When considering all species of terrestrial mammals occurring in present cropland regions (n=3922), the average gains decrease to 7.6% under the TLS scenario and increase to 4.9% in the MLS scenario (see Supplementary Figure S17 for results on various species groups). The effect in the TLS scenario is partly due to the fact that cropland is spared therein specifically for small-range species. The modest gain in average habitat for all terrestrial mammals in the MLS scenario in turn reflects that cropland presently covers about 10% of the global ice-free land surface and therefore only a comparably small fraction of actual and potential natural vegetation. Thus, our results underpin that land sparing is most effective if pursued in a targeted way and focused on species strongly affected by conversion of natural vegetation to cropland.

Our assessment of potential biodiversity impacts quantifies changes in suitable habitat area for species intolerant to cropland, a time-independent indicator free of assumptions on population dynamics and applicable for a wide range of species<sup>44,45</sup>. Yet, this neglects potential impacts of intensification on biodiversity *in situ* on cropland. The bulk of empirical studies on species density-crop yield relationships found that these follow a negatively convex functional form for species sensitive to cropland with rapidly decreasing species density already at low yields<sup>46</sup>. This favours land sparing as a conservation strategy opposed to land sharing or wildlife-friendly farming. The abundance of species tolerant to cropland in turn may depend on multiple factors such as crop diversity and field configuration, nutrient inputs, pesticide applications, small-scale landscape configuration, and species' sensitivities to these aspects<sup>47</sup>. Due to lack of data and granular spatial resolutions, these aspects cannot be addressed herein and hardly in global studies at present. Indications that substantial land sparing can be achieved with sustainable intensification in some regions but less so in others is provided in the evaluation of crop diversity and nutrient budgets above. Yet, local assessments employing detailed species- and ecosystem-specific knowledge will be required to explicitly quantify such effects.

In summary, both land sparing scenarios entail various co-benefits along agro-environmental dimensions. Thereby, the targeted land sparing approach not only allows for the implicitly higher habitat restoration potential, but also lower nutrient requirements and higher C sequestration potential, although differences between scenarios are often marginal. As all modelling studies, our findings are subject to a range of uncertainties and limitations, which we consider to render our results conservative rather than overly optimistic (Supplementary Text S3 and S4).

## **Conclusions and wider implications of extensive land sparing**

The potential for cropland sparing quantified herein contrasts with earlier agro-economic studies indicating that further cropland expansion is likely to occur in future decades due to increasing crop demands and slow diffusion rates of agricultural technologies<sup>13,48,49</sup>. Noteworthy, these forward-looking studies account for changes in climate and atmospheric CO<sub>2</sub> concentration as well as socio-economic drivers and constraints, including diffusion rates for improved agricultural technologies, national agricultural policies, international trade relations, and future increases in demands, which limit their comparability to ours. Earlier studies exploring combinations of biophysical and socio-economic options for abating increasing land pressure of agricultural production already identified agro-technologic change as an important element<sup>15,16</sup> but presented compound scenarios that do not allow for quantifying the land sparing potential of optimal crop production and associated externalities directly. Quantifications of production potentials<sup>17–21</sup> in turn do not consider actual crop demands and none of the mentioned studies covered targeted land sparing for wildlife habitats and other landscape elements. In this context, our results provide a benchmark of the present potential for cropland sparing if high land use efficiency was realized and if specific targets are defined for restoring wildlife habitats.

The gap between the present extent of global cropland and the actual cropland requirement quantified herein indicates that at the global scale land management and associated policies, rather than biophysical limitations, are the major production-side drivers of adverse environmental change mediated by the expansion of cropland<sup>48</sup>. Thus, achieving ambitious land sparing targets in the near term will require radical acceleration in the dissemination of available agro-technologies as well as integration across society<sup>31</sup> to avoid cropland expansion often caused by sole incentives for intensification<sup>7</sup> while maintaining livelihoods of populations potentially affected by agricultural change. Globally coordinated efforts<sup>50</sup> will be required to balance national interests concerning food security and agricultural revenues with global environmental targets.

## Methods and Data

### Study design and land sparing scenarios

The study investigated global cropland sparing potential based on crop modelling of attainable yields for 16 major crops, crop-specific land use datasets, and spatial optimization of cropland allocation (Figure 1) to minimize global cropland extent via maximizing land use efficiency, i.e. assigning the most productive crops to cropland locally. The considered crops represent 85% of global cropland cultivated with annual crops and sum up to more than 75% of total cropland area, vegetal calorie supply, and fertilizer consumption<sup>29</sup>. With the exceptions of cassava and sugarcane, we excluded perennial crops from our analyses, due to their low flexibility for crop switching and specific trajectories of yield improvement. Within the optimization algorithm, current crop-specific area may expand or shrink with the goal of minimizing global cropland extent, while maintaining defined crop-specific production volumes reported by FAO for 2011-2015<sup>29</sup> and without expanding total cropland extent locally. We opted for the most recent period for which data are available to account for contemporary increases in crop production. The five-year mean is a compromise between avoiding bias from selecting a single year and underestimating present production volumes when using a longer historical period. The study design is further detailed in Supplementary Methods S1 and visualized in Figure 1.

We evaluated cropland sparing potential for two distinct main scenarios: (i) the “maximum land sparing” (MLS) potential allowing the entire present cropland in each simulation unit or pixel to remain occupied after crop reallocation if it is a solution of the optimization, and (ii) a “targeted land sparing” (TLS) scenario. The latter forces the release of all cropland covered by the considered crops in biodiversity hotspots and a uniform release of at least 20% of present cropland cover by 16 major crops in each simulation unit or pixel. The latter fraction is considered to spare a compartment of the landscape for other, i.e. regenerative, uses. Herein, it is assumed to be covered by natural vegetation in the quantification of externalities (carbon sequestration and area of habitat), but may in principle also serve for buffer strips, windbreaks, or other landscape elements.

Two supplementary scenarios based on the MLS scenario (Figure 1E) provide additional information (I) whether the cultivation of crops in regions in which their cultivation is presently not recorded plays a major role in the land sparing potential found herein, which is termed “MLS without crop switching” (MLS<sub>nsc</sub>); and (II) if substantial cropland sparing is still feasible if single crops are allowed to only cover ≤34% of cropland in each simulation unit, indirectly enforcing the occurrence of several crops in most simulation units and hence fostering crop diversity, which allows for crop rotations. This scenario is termed “MLS with crop diversity” (MLS<sub>wcd</sub>).

Land use optimization approaches similar to the main scenarios have been studied earlier, but addressed global production potentials employing input intensification only<sup>19</sup>, crop switching only<sup>20,21</sup>, or both<sup>18</sup>, or investigated production potentials for single crops under climate change<sup>17</sup>. Land sparing potential of optimized cropland allocation has been addressed by Müller et al.<sup>51</sup> among other aspects of crop production and consumption. Yet, constraints on available land for cropping per pixel were not considered below the physical pixel area, crop demands were partly computed, and intensification was not accounted for.

### Crop modelling framework

Crop simulations were performed for 16 major crops (Figure 2) with the well-established global gridded crop model (GGCM) EPIC-IIASA<sup>17</sup>, which is based on the field-scale process-based agronomic Environmental Policy Integrated Climate (EPIC) model<sup>25,26</sup> (formerly known as Erosion Productivity Impact Calculator). EPIC-IIASA has been applied extensively in global impact studies and across regions, and has been evaluated positively for reproducing both historic absolute yields under business-as-usual management and inter-annual yield variability<sup>52–54</sup>. Simulated attainable crop yields were capped at the 95<sup>th</sup> percentile globally to avoid bias towards extremely high yields in the crop-to-cropland allocation. Key processes of the core model EPIC are summarized in Folberth et al.<sup>55</sup> and briefly described in Supplementary Methods S3.

EPIC-IIASA is based on a 5 x 5' grid (equivalent to about 8.3 km x 8.3 km near the equator) for soil characteristics<sup>56</sup> and topography<sup>57</sup> that are aggregated, based on classification of key characteristics, to homogenous response units. These are further intersected using a 30 x 30' climate grid (about 50 km x 50 km near the equator) and national administrative boundaries to define final simulation units<sup>58</sup>. Accordingly, simulation units vary in size from 5' x 5' to 30' x 30' depending on local heterogeneity. More detail on the definition of simulation units is provided in Supplementary Methods S2. The EPIC model was run for each simulation unit, crop, and water management system (rainfed or with sufficient irrigation) separately, treating it as a representative homogenous field. Climate data were based on the daily climate database AgMERRA<sup>59</sup>, specifically developed for agricultural applications, at a spatial resolution of 30' x 30'. Crop-specific growing seasons were derived from Sacks et al.<sup>60</sup>. Supplementary Methods S2 provide further details on the EPIC-IIASA model.

Data on multi-cropping are lacking at the global scale and are only reflected in reported harvest areas that partly exceed the physical area of cropland. As our focus was on physical cropland sparing, we focused our optimization on single cropping of physical cropland, disregarding potential multi-cropping and rotations. The exception was for rice cultivation: according to SPAM 2005 v3.2<sup>61</sup>, total cropping intensity is about 115%, with single cropping dominant in most crops, but an intensity of 150% for rice. Therefore, rice was simulated for two seasons where suggested by calendar data, to minimize underestimation of rice double cropping. Yields for the two seasons were summed to treat double-cropped rice as a single crop in the estimation of physical area requirements. For the land use datasets referring to harvested area (see below), separate rice simulations were performed for a single season. A brief discussion of the potential impacts of multi-cropping is provided in Supplementary Text S4.

## **Evaluation of attainable crop yields**

We evaluated simulated attainable yields against two widely used spatially explicit datasets, based on reported yields and extrapolation of (a) high-input rainfed and irrigated crop yields from SPAM 2005 v3.2<sup>61</sup> and (b) attainable yields<sup>19</sup> based on the M3 dataset<sup>19</sup>. Evaluations are presented in Supplementary Text S2 and Supplementary Figures S12 and S14. All three datasets (including the estimates from biophysical crop modelling) were derived using different methodologies; this limits comparability of yield distributions. It may be assumed, however, that our comparison allows for the evaluation of crop model overestimation of yield potentials. It should be noted that the yield category closest to attainable yields in SPAM reports rainfed, high-input yields, based on moderate to sufficient levels of nutrient input. Irrigated yields are a single category that may typically be assumed to receive high (unknown) levels of nutrient inputs. The attainable yields from M3 are based on spatially explicit reported yields c. 2000 from administrative level censuses and climate bins based on temperature and precipitation. For

each of these climate bins, the upper 95<sup>th</sup> percentile of reported yields is assumed to represent the attainable yield.

### Cropland allocation model

Spatially explicit cropland optimization was performed at the level of simulation units with the objective of minimizing global cropland requirement, but maintaining 2011-2015 production volumes for each crop<sup>29</sup> (Figure 1). Reported production as a target accounts for any dietary and other use preferences as opposed to more aggregated approaches based on recommended supply levels or requirements.

The main cropland dataset selected for the analysis was SPAM 2005 v3.2, because it provides crop-specific physical areas. In contrast to other datasets that typically report either crop-specific harvested areas or total physical cropland, this dataset allows for the assessment of physical cropland sparing potential only for cropland cultivated with the crops included in this analysis. Robustness of our results was evaluated from the optimization of two additional crop-specific harvested area datasets (see below).

The land use optimization model was programmed in GAMS software (<https://gams.com/>), where input data are yield potentials from either the EPIC crop model or inventory data (see below) and current crop-specific areas at the simulation unit level. Thresholds for uniform cropland release in the TLS scenario were defined by finding a minimal feasible solution in steps of 85%, 80%, 67%, and 50% for each attainable crop yield x cropland dataset combination. For the SPAM 2005 physical area dataset, this threshold was found to be 80% (or 20% of uniformly released land).

The optimization problem is formulated as:

$$\min \sum_i \sum_j \sum_k \sum_l \sum_m \sum_n \sum_o \sum_p \sum_q \sum_r \sum_s \sum_t \sum_u \sum_v \sum_w \sum_x \sum_y \sum_z \sum_{aa} \sum_{ab} \sum_{ac} \sum_{ad} \sum_{ae} \sum_{af} \sum_{ag} \sum_{ah} \sum_{ai} \sum_{aj} \sum_{ak} \sum_{al} \sum_{am} \sum_{an} \sum_{ao} \sum_{ap} \sum_{aq} \sum_{ar} \sum_{as} \sum_{at} \sum_{au} \sum_{av} \sum_{aw} \sum_{ax} \sum_{ay} \sum_{az} \sum_{ba} \sum_{bb} \sum_{bc} \sum_{bd} \sum_{be} \sum_{bf} \sum_{bg} \sum_{bh} \sum_{bi} \sum_{bj} \sum_{bk} \sum_{bl} \sum_{bm} \sum_{bn} \sum_{bo} \sum_{bp} \sum_{bq} \sum_{br} \sum_{bs} \sum_{bt} \sum_{bu} \sum_{bv} \sum_{bw} \sum_{bx} \sum_{by} \sum_{bz} \sum_{ca} \sum_{cb} \sum_{cc} \sum_{cd} \sum_{ce} \sum_{cf} \sum_{cg} \sum_{ch} \sum_{ci} \sum_{cj} \sum_{ck} \sum_{cl} \sum_{cm} \sum_{cn} \sum_{co} \sum_{cp} \sum_{cq} \sum_{cr} \sum_{cs} \sum_{ct} \sum_{cu} \sum_{cv} \sum_{cw} \sum_{cx} \sum_{cy} \sum_{cz} \sum_{da} \sum_{db} \sum_{dc} \sum_{dd} \sum_{de} \sum_{df} \sum_{dg} \sum_{dh} \sum_{di} \sum_{dj} \sum_{dk} \sum_{dl} \sum_{dm} \sum_{dn} \sum_{do} \sum_{dp} \sum_{dq} \sum_{dr} \sum_{ds} \sum_{dt} \sum_{du} \sum_{dv} \sum_{dw} \sum_{dx} \sum_{dy} \sum_{dz} \sum_{ea} \sum_{eb} \sum_{ec} \sum_{ed} \sum_{ee} \sum_{ef} \sum_{eg} \sum_{eh} \sum_{ei} \sum_{ej} \sum_{ek} \sum_{el} \sum_{em} \sum_{en} \sum_{eo} \sum_{ep} \sum_{eq} \sum_{er} \sum_{es} \sum_{et} \sum_{eu} \sum_{ev} \sum_{ew} \sum_{ex} \sum_{ey} \sum_{ez} \sum_{fa} \sum_{fb} \sum_{fc} \sum_{fd} \sum_{fe} \sum_{ff} \sum_{fg} \sum_{fh} \sum_{fi} \sum_{fj} \sum_{fk} \sum_{fl} \sum_{fm} \sum_{fn} \sum_{fo} \sum_{fp} \sum_{fq} \sum_{fr} \sum_{fs} \sum_{ft} \sum_{fu} \sum_{fv} \sum_{fw} \sum_{fx} \sum_{fy} \sum_{fz} \sum_{ga} \sum_{gb} \sum_{gc} \sum_{gd} \sum_{ge} \sum_{gf} \sum_{gg} \sum_{gh} \sum_{gi} \sum_{gj} \sum_{gk} \sum_{gl} \sum_{gm} \sum_{gn} \sum_{go} \sum_{gp} \sum_{gq} \sum_{gr} \sum_{gs} \sum_{gt} \sum_{gu} \sum_{gv} \sum_{gw} \sum_{gx} \sum_{gy} \sum_{gz} \sum_{ha} \sum_{hb} \sum_{hc} \sum_{hd} \sum_{he} \sum_{hf} \sum_{hg} \sum_{hh} \sum_{hi} \sum_{hj} \sum_{hk} \sum_{hl} \sum_{hm} \sum_{hn} \sum_{ho} \sum_{hp} \sum_{hq} \sum_{hr} \sum_{hs} \sum_{ht} \sum_{hu} \sum_{hv} \sum_{hw} \sum_{hx} \sum_{hy} \sum_{hz} \sum_{ia} \sum_{ib} \sum_{ic} \sum_{id} \sum_{ie} \sum_{if} \sum_{ig} \sum_{ih} \sum_{ii} \sum_{ij} \sum_{ik} \sum_{il} \sum_{im} \sum_{in} \sum_{io} \sum_{ip} \sum_{iq} \sum_{ir} \sum_{is} \sum_{it} \sum_{iu} \sum_{iv} \sum_{iw} \sum_{ix} \sum_{iy} \sum_{iz} \sum_{ja} \sum_{jb} \sum_{jc} \sum_{jd} \sum_{je} \sum_{jf} \sum_{jg} \sum_{jh} \sum_{ji} \sum_{jj} \sum_{jk} \sum_{jl} \sum_{jm} \sum_{jn} \sum_{jo} \sum_{jp} \sum_{jq} \sum_{jr} \sum_{js} \sum_{jt} \sum_{ju} \sum_{jv} \sum_{jw} \sum_{jx} \sum_{jy} \sum_{jz} \sum_{ka} \sum_{kb} \sum_{kc} \sum_{kd} \sum_{ke} \sum_{kf} \sum_{kg} \sum_{kh} \sum_{ki} \sum_{kj} \sum_{kk} \sum_{kl} \sum_{km} \sum_{kn} \sum_{ko} \sum_{kp} \sum_{kq} \sum_{kr} \sum_{ks} \sum_{kt} \sum_{ku} \sum_{kv} \sum_{kw} \sum_{kx} \sum_{ky} \sum_{kz} \sum_{la} \sum_{lb} \sum_{lc} \sum_{ld} \sum_{le} \sum_{lf} \sum_{lg} \sum_{lh} \sum_{li} \sum_{lj} \sum_{lk} \sum_{ll} \sum_{lm} \sum_{ln} \sum_{lo} \sum_{lp} \sum_{lq} \sum_{lr} \sum_{ls} \sum_{lt} \sum_{lu} \sum_{lv} \sum_{lw} \sum_{lx} \sum_{ly} \sum_{lz} \sum_{ma} \sum_{mb} \sum_{mc} \sum_{md} \sum_{me} \sum_{mf} \sum_{mg} \sum_{mh} \sum_{mi} \sum_{mj} \sum_{mk} \sum_{ml} \sum_{mm} \sum_{mn} \sum_{mo} \sum_{mp} \sum_{mq} \sum_{mr} \sum_{ms} \sum_{mt} \sum_{mu} \sum_{mv} \sum_{mw} \sum_{mx} \sum_{my} \sum_{mz} \sum_{na} \sum_{nb} \sum_{nc} \sum_{nd} \sum_{ne} \sum_{nf} \sum_{ng} \sum_{nh} \sum_{ni} \sum_{nj} \sum_{nk} \sum_{nl} \sum_{nm} \sum_{nn} \sum_{no} \sum_{np} \sum_{nq} \sum_{nr} \sum_{ns} \sum_{nt} \sum_{nu} \sum_{nv} \sum_{nw} \sum_{nx} \sum_{ny} \sum_{nz} \sum_{oa} \sum_{ob} \sum_{oc} \sum_{od} \sum_{oe} \sum_{of} \sum_{og} \sum_{oh} \sum_{oi} \sum_{oj} \sum_{ok} \sum_{ol} \sum_{om} \sum_{on} \sum_{oo} \sum_{op} \sum_{oq} \sum_{or} \sum_{os} \sum_{ot} \sum_{ou} \sum_{ov} \sum_{ow} \sum_{ox} \sum_{oy} \sum_{oz} \sum_{pa} \sum_{pb} \sum_{pc} \sum_{pd} \sum_{pe} \sum_{pf} \sum_{pg} \sum_{ph} \sum_{pi} \sum_{pj} \sum_{pk} \sum_{pl} \sum_{pm} \sum_{pn} \sum_{po} \sum_{pp} \sum_{pq} \sum_{pr} \sum_{ps} \sum_{pt} \sum_{pu} \sum_{pv} \sum_{pw} \sum_{px} \sum_{py} \sum_{pz} \sum_{qa} \sum_{qb} \sum_{qc} \sum_{qd} \sum_{qe} \sum_{qf} \sum_{qg} \sum_{qh} \sum_{qi} \sum_{qj} \sum_{qk} \sum_{ql} \sum_{qm} \sum_{qn} \sum_{qo} \sum_{qp} \sum_{qq} \sum_{qr} \sum_{qs} \sum_{qt} \sum_{qu} \sum_{qv} \sum_{qw} \sum_{qx} \sum_{qy} \sum_{qz} \sum_{ra} \sum_{rb} \sum_{rc} \sum_{rd} \sum_{re} \sum_{rf} \sum_{rg} \sum_{rh} \sum_{ri} \sum_{rj} \sum_{rk} \sum_{rl} \sum_{rm} \sum_{rn} \sum_{ro} \sum_{rp} \sum_{rq} \sum_{rr} \sum_{rs} \sum_{rt} \sum_{ru} \sum_{rv} \sum_{rw} \sum_{rx} \sum_{ry} \sum_{rz} \sum_{sa} \sum_{sb} \sum_{sc} \sum_{sd} \sum_{se} \sum_{sf} \sum_{sg} \sum_{sh} \sum_{si} \sum_{sj} \sum_{sk} \sum_{sl} \sum_{sm} \sum_{sn} \sum_{so} \sum_{sp} \sum_{sq} \sum_{sr} \sum_{ss} \sum_{st} \sum_{su} \sum_{sv} \sum_{sw} \sum_{sx} \sum_{sy} \sum_{sz} \sum_{ta} \sum_{tb} \sum_{tc} \sum_{td} \sum_{te} \sum_{tf} \sum_{tg} \sum_{th} \sum_{ti} \sum_{tj} \sum_{tk} \sum_{tl} \sum_{tm} \sum_{tn} \sum_{to} \sum_{tp} \sum_{tq} \sum_{tr} \sum_{ts} \sum_{tt} \sum_{tu} \sum_{tv} \sum_{tw} \sum_{tx} \sum_{ty} \sum_{tz} \sum_{ua} \sum_{ub} \sum_{uc} \sum_{ud} \sum_{ue} \sum_{uf} \sum_{ug} \sum_{uh} \sum_{ui} \sum_{uj} \sum_{uk} \sum_{ul} \sum_{um} \sum_{un} \sum_{uo} \sum_{up} \sum_{uq} \sum_{ur} \sum_{us} \sum_{ut} \sum_{uu} \sum_{uv} \sum_{uw} \sum_{ux} \sum_{uy} \sum_{uz} \sum_{va} \sum_{vb} \sum_{vc} \sum_{vd} \sum_{ve} \sum_{vf} \sum_{vg} \sum_{vh} \sum_{vi} \sum_{vj} \sum_{vk} \sum_{vl} \sum_{vm} \sum_{vn} \sum_{vo} \sum_{vp} \sum_{vq} \sum_{vr} \sum_{vs} \sum_{vt} \sum_{vu} \sum_{vv} \sum_{vw} \sum_{vx} \sum_{vy} \sum_{vz} \sum_{wa} \sum_{wb} \sum_{wc} \sum_{wd} \sum_{we} \sum_{wf} \sum_{wg} \sum_{wh} \sum_{wi} \sum_{wj} \sum_{wk} \sum_{wl} \sum_{wm} \sum_{wn} \sum_{wo} \sum_{wp} \sum_{wq} \sum_{wr} \sum_{ws} \sum_{wt} \sum_{wu} \sum_{wv} \sum_{ww} \sum_{wx} \sum_{wy} \sum_{wz} \sum_{xa} \sum_{xb} \sum_{xc} \sum_{xd} \sum_{xe} \sum_{xf} \sum_{xg} \sum_{xh} \sum_{xi} \sum_{xj} \sum_{xk} \sum_{xl} \sum_{xm} \sum_{xn} \sum_{xo} \sum_{xp} \sum_{xq} \sum_{xr} \sum_{xs} \sum_{xt} \sum_{xu} \sum_{xv} \sum_{xw} \sum_{xx} \sum_{xy} \sum_{xz} \sum_{ya} \sum_{yb} \sum_{yc} \sum_{yd} \sum_{ye} \sum_{yf} \sum_{yg} \sum_{yh} \sum_{yi} \sum_{yj} \sum_{yk} \sum_{yl} \sum_{ym} \sum_{yn} \sum_{yo} \sum_{yp} \sum_{yq} \sum_{yr} \sum_{ys} \sum_{yt} \sum_{yu} \sum_{yv} \sum_{yw} \sum_{yx} \sum_{yy} \sum_{yz} \sum_{za} \sum_{zb} \sum_{zc} \sum_{zd} \sum_{ze} \sum_{zf} \sum_{zg} \sum_{zh} \sum_{zi} \sum_{zj} \sum_{zk} \sum_{zl} \sum_{zm} \sum_{zn} \sum_{zo} \sum_{zp} \sum_{zq} \sum_{zr} \sum_{zs} \sum_{zt} \sum_{zu} \sum_{zv} \sum_{zw} \sum_{zx} \sum_{zy} \sum_{zz} \sum_{aa} \sum_{ab} \sum_{ac} \sum_{ad} \sum_{ae} \sum_{af} \sum_{ag} \sum_{ah} \sum_{ai} \sum_{aj} \sum_{ak} \sum_{al} \sum_{am} \sum_{an} \sum_{ao} \sum_{ap} \sum_{aq} \sum_{ar} \sum_{as} \sum_{at} \sum_{au} \sum_{av} \sum_{aw} \sum_{ax} \sum_{ay} \sum_{az} \sum_{ba} \sum_{bb} \sum_{bc} \sum_{bd} \sum_{be} \sum_{bf} \sum_{bg} \sum_{bh} \sum_{bi} \sum_{bj} \sum_{bk} \sum_{bl} \sum_{bm} \sum_{bn} \sum_{bo} \sum_{bp} \sum_{bq} \sum_{br} \sum_{bs} \sum_{bt} \sum_{bu} \sum_{bv} \sum_{bw} \sum_{bx} \sum_{by} \sum_{bz} \sum_{ca} \sum_{cb} \sum_{cc} \sum_{cd} \sum_{ce} \sum_{cf} \sum_{cg} \sum_{ch} \sum_{ci} \sum_{cj} \sum_{ck} \sum_{cl} \sum_{cm} \sum_{cn} \sum_{co} \sum_{cp} \sum_{cq} \sum_{cr} \sum_{cs} \sum_{ct} \sum_{cu} \sum_{cv} \sum_{cw} \sum_{cx} \sum_{cy} \sum_{cz} \sum_{da} \sum_{db} \sum_{dc} \sum_{dd} \sum_{de} \sum_{df} \sum_{dg} \sum_{dh} \sum_{di} \sum_{dj} \sum_{dk} \sum_{dl} \sum_{dm} \sum_{dn} \sum_{do} \sum_{dp} \sum_{dq} \sum_{dr} \sum_{ds} \sum_{dt} \sum_{du} \sum_{dv} \sum_{dw} \sum_{dx} \sum_{dy} \sum_{dz} \sum_{ea} \sum_{eb} \sum_{ec} \sum_{ed} \sum_{ee} \sum_{ef} \sum_{eg} \sum_{eh} \sum_{ei} \sum_{ej} \sum_{ek} \sum_{el} \sum_{em} \sum_{en} \sum_{eo} \sum_{ep} \sum_{eq} \sum_{er} \sum_{es} \sum_{et} \sum_{eu} \sum_{ev} \sum_{ew} \sum_{ex} \sum_{ey} \sum_{ez} \sum_{fa} \sum_{fb} \sum_{fc} \sum_{fd} \sum_{fe} \sum_{ff} \sum_{fg} \sum_{fh} \sum_{fi} \sum_{fj} \sum_{fk} \sum_{fl} \sum_{fm} \sum_{fn} \sum_{fo} \sum_{fp} \sum_{fq} \sum_{fr} \sum_{fs} \sum_{ft} \sum_{fu} \sum_{fv} \sum_{fw} \sum_{fx} \sum_{fy} \sum_{fz} \sum_{ga} \sum_{gb} \sum_{gc} \sum_{gd} \sum_{ge} \sum_{gf} \sum_{gg} \sum_{gh} \sum_{gi} \sum_{gj} \sum_{gk} \sum_{gl} \sum_{gm} \sum_{gn} \sum_{go} \sum_{gp} \sum_{gq} \sum_{gr} \sum_{gs} \sum_{gt} \sum_{gu} \sum_{gv} \sum_{gw} \sum_{gx} \sum_{gy} \sum_{gz} \sum_{ha} \sum_{hb} \sum_{hc} \sum_{hd} \sum_{he} \sum_{hf} \sum_{hg} \sum_{hh} \sum_{hi} \sum_{hj} \sum_{hk} \sum_{hl} \sum_{hm} \sum_{hn} \sum_{ho} \sum_{hp} \sum_{hq} \sum_{hr} \sum_{hs} \sum_{ht} \sum_{hu} \sum_{hv} \sum_{hw} \sum_{hx} \sum_{hy} \sum_{hz} \sum_{ia} \sum_{ib} \sum_{ic} \sum_{id} \sum_{ie} \sum_{if} \sum_{ig} \sum_{ih} \sum_{ii} \sum_{ij} \sum_{ik} \sum_{il} \sum_{im} \sum_{in} \sum_{io} \sum_{ip} \sum_{iq} \sum_{ir} \sum_{is} \sum_{it} \sum_{iu} \sum_{iv} \sum_{iw} \sum_{ix} \sum_{iy} \sum_{iz} \sum_{ja} \sum_{jb} \sum_{jc} \sum_{jd} \sum_{je} \sum_{jf} \sum_{jg} \sum_{jh} \sum_{ji} \sum_{jj} \sum_{jk} \sum_{jl} \sum_{jm} \sum_{jn} \sum_{jo} \sum_{jp} \sum_{jq} \sum_{jr} \sum_{js} \sum_{jt} \sum_{ju} \sum_{jv} \sum_{jw} \sum_{jx} \sum_{jy} \sum_{jz} \sum_{ka} \sum_{kb} \sum_{kc} \sum_{kd} \sum_{ke} \sum_{kf} \sum_{kg} \sum_{kh} \sum_{ki} \sum_{kj} \sum_{kk} \sum_{kl} \sum_{km} \sum_{kn} \sum_{ko} \sum_{kp} \sum_{kq} \sum_{kr} \sum_{ks} \sum_{kt} \sum_{ku} \sum_{kv} \sum_{kw} \sum_{kx} \sum_{ky} \sum_{kz} \sum_{la} \sum_{lb} \sum_{lc} \sum_{ld} \sum_{le} \sum_{lf} \sum_{lg} \sum_{lh} \sum_{li} \sum_{lj} \sum_{lk} \sum_{ll} \sum_{lm} \sum_{ln} \sum_{lo} \sum_{lp} \sum_{lq} \sum_{lr} \sum_{ls} \sum_{lt} \sum_{lu} \sum_{lv} \sum_{lw} \sum_{lx} \sum_{ly} \sum_{lz} \sum_{ma} \sum_{mb} \sum_{mc} \sum_{md} \sum_{me} \sum_{mf} \sum_{mg} \sum_{mh} \sum_{mi} \sum_{mj} \sum_{mk} \sum_{ml} \sum_{mm} \sum_{mn} \sum_{mo} \sum_{mp} \sum_{mq} \sum_{mr} \sum_{ms} \sum_{mt} \sum_{mu} \sum_{mv} \sum_{mw} \sum_{mx} \sum_{my} \sum_{mz} \sum_{na} \sum_{nb} \sum_{nc} \sum_{nd} \sum_{ne} \sum_{nf} \sum_{ng} \sum_{nh} \sum_{ni} \sum_{nj} \sum_{nk} \sum_{nl} \sum_{nm} \sum_{nn} \sum_{no} \sum_{np} \sum_{nq} \sum_{nr} \sum_{ns} \sum_{nt} \sum_{nu} \sum_{nv} \sum_{nw} \sum_{nx} \sum_{ny} \sum_{nz} \sum_{oa} \sum_{ob} \sum_{oc} \sum_{od} \sum_{oe} \sum_{of} \sum_{og} \sum_{oh} \sum_{oi} \sum_{oj} \sum_{ok} \sum_{ol} \sum_{om} \sum_{on} \sum_{oo} \sum_{op} \sum_{oq} \sum_{or} \sum_{os} \sum_{ot} \sum_{ou} \sum_{ov} \sum_{ow} \sum_{ox} \sum_{oy} \sum_{oz} \sum_{pa} \sum_{pb} \sum_{pc} \sum_{pd} \sum_{pe} \sum_{pf} \sum_{pg} \sum_{ph} \sum_{pi} \sum_{pj} \sum_{pk} \sum_{pl} \sum_{pm} \sum_{pn} \sum_{po} \sum_{pp} \sum_{pq} \sum_{pr} \sum_{ps} \sum_{pt} \sum_{pu} \sum_{pv} \sum_{pw} \sum_{px} \sum_{py} \sum_{pz} \sum_{qa} \sum_{qb} \sum_{qc} \sum_{qd} \sum_{qe} \sum_{qf} \sum_{qg} \sum_{qh} \sum_{qi} \sum_{qj} \sum_{qk} \sum_{ql} \sum_{qm} \sum_{qn} \sum_{qo} \sum_{qp} \sum_{qq} \sum_{qr} \sum_{qs} \sum_{qt} \sum_{qu} \sum_{qv} \sum_{qw} \sum_{qx} \sum_{qy} \sum_{qz} \sum_{ra} \sum_{rb} \sum_{rc} \sum_{rd} \sum_{re} \sum_{rf} \sum_{rg} \sum_{rh} \sum_{ri} \sum_{rj} \sum_{rk} \sum_{rl} \sum_{rm} \sum_{rn} \sum_{ro} \sum_{rp} \sum_{rq} \sum_{rr} \sum_{rs} \sum_{rt} \sum_{ru} \sum_{rv} \sum_{rw} \sum_{rx} \sum_{ry} \sum_{rz} \sum_{sa} \sum_{sb} \sum_{sc} \sum_{sd} \sum_{se} \sum_{sf} \sum_{sg} \sum_{sh} \sum_{si} \sum_{sj} \sum_{sk} \sum_{sl} \sum_{sm} \sum_{sn} \sum_{so} \sum_{sp} \sum_{sq} \sum_{sr} \sum_{ss} \sum_{st} \sum_{su} \sum_{sv} \sum_{sw} \sum_{sx} \sum_{sy} \sum_{sz} \sum_{ta} \sum_{tb} \sum_{tc} \sum_{td} \sum_{te} \sum_{tf} \sum_{tg} \sum_{th} \sum_{ti} \sum_{tj} \sum_{tk} \sum_{tl} \sum_{tm} \sum_{tn} \sum_{to} \sum_{tp} \sum_{tq} \sum_{tr} \sum_{ts} \sum_{tt} \sum_{tu} \sum_{tv} \sum_{tw} \sum_{tx} \sum_{ty} \sum_{tz} \sum_{ua} \sum_{ub} \sum_{uc} \sum_{ud} \sum_{ue} \sum_{uf} \sum_{ug} \sum_{uh} \sum_{ui} \sum_{uj} \sum_{uk} \sum_{ul} \sum_{um} \sum_{un} \sum_{uo} \sum_{up} \sum_{uq} \sum_{ur} \sum_{us} \sum_{ut} \sum_{uu} \sum_{uv} \sum_{uw} \sum_{ux} \sum_{uy} \sum_{uz} \sum_{va} \sum_{vb} \sum_{vc} \sum_{vd} \sum_{ve} \sum_{vf} \sum_{vg} \sum_{vh} \sum_{vi} \sum_{vj} \sum_{vk} \sum_{vl} \sum_{vm} \sum_{vn} \sum_{vo} \sum_{vp} \sum_{vq} \sum_{vr} \sum_{vs} \sum_{vt} \sum_{vu} \sum_{vv} \sum_{vw} \sum_{vx} \sum_{vy} \sum_{vz} \sum_{wa} \sum_{wb} \sum_{wc} \sum_{wd} \sum_{we} \sum_{wf} \sum_{wg} \sum_{wh} \sum_{wi} \sum_{wj} \sum_{wk} \sum_{wl} \sum_{wm} \sum_{wn} \sum_{wo} \sum_{wp} \sum_{wq} \sum_{wr} \sum_{ws} \sum_{wt} \sum_{wu} \sum_{wv} \sum_{ww} \sum_{wx} \sum_{wy} \sum_{wz} \sum_{xa} \sum_{xb} \sum_{xc} \sum_{xd} \sum_{xe} \sum_{xf} \sum_{xg} \sum_{xh} \sum_{xi} \sum_{xj} \sum_{xk} \sum_{xl} \sum_{xm} \sum_{xn} \sum_{xo} \sum_{xp} \sum_{xq} \sum_{xr} \sum_{xs} \sum_{xt} \sum_{xu} \sum_{xv} \sum_{xw} \sum_{xx} \sum_{xy} \sum_{xz} \sum_{ya} \sum_{yb} \sum_{yc} \sum_{yd} \sum_{ye} \sum_{yf} \sum_{yg} \sum_{yh} \sum_{yi} \sum_{yj} \sum_{yk} \sum_{yl} \sum_{ym} \sum_{yn} \sum_{yo} \sum_{yp} \sum_{yq} \sum_{yr} \sum_{ys} \sum_{yt} \sum_{yu} \sum_{yv} \sum_{yw} \sum_{yx} \sum_{yy} \sum_{yz} \sum_{za} \sum_{zb} \sum_{zc} \sum_{zd} \sum_{ze} \sum_{zf} \sum_{zg} \sum_{zh} \sum_{zi} \sum_{zj} \sum_{zk} \sum_{zl} \sum_{zm} \sum_{zn} \sum_{zo} \sum_{zp} \sum_{zq} \sum_{zr} \sum_{zs} \sum_{zt} \sum_{zu} \sum_{zv} \sum_{zw} \sum_{zx} \sum_{zy} \sum_{zz}$$

(Eq. 1)

$$\dots$$

(Eq. 2)

$$\dots$$

(Eq. 3)

where  $A_{i,j}$  is current area of cropland [ha] occupied by the considered crops in simulation unit  $i$  under water supply type  $j$ ;  $\alpha_{i,j}$  is the respective share allocated to crop  $k$  to be optimized;  $Y_{i,j,k}$  is the simulation unit-, irrigation type-, and crop-specific yield [t ha<sup>-1</sup>];  $P_{i,j,k}$  is current production<sup>23</sup> of crop  $k$  [t];  $A_{i,j,k}^{\max}$  is the maximum allowed optimized cropland share within the considered simulation unit area, for maximum land sparing; and  $A_{i,j,k}^{\max}$  for SPAM for the TLS scenario. For the complementary datasets (see below),  $A_{i,j,k}^{\max}$  for MIRCA, and  $A_{i,j,k}^{\max}$  85 for the M3 dataset.

We performed optimizations for additional datasets and combinations thereof to account for uncertainties in cropland distribution<sup>62</sup> and attainable yields. Crop model estimated attainable yields were combined with cropland distributions from SPAM 2005 v3.2<sup>61</sup> or MIRCA2000<sup>63</sup> that provide spatially explicit harvested areas for the considered crops, for rainfed and irrigated cultivation systems separately. We performed the same complementary optimization using a set of statistically derived attainable yields and corresponding areas from M3<sup>19,64</sup>; this dataset does not distinguish between rainfed and irrigated systems, so yields were not combined with the other land use datasets. As none of the spatial datasets provides the same crop-specific areas as FAOSTAT for the reference period 2011-

2015<sup>23</sup>, crop areas from FAOSTAT were used as a basis from which to derive relative cropland area reduction, after an absolute number of cropland requirement had been obtained in the optimization routine. Accordingly, cropland areas in all spatial datasets underestimate present cropland, which increased for the considered crops by about 14% since 2000 (M3 and MIRCA2000 reference), and by 7% since 2005 (SPAM 2005 reference). Further limitations and uncertainties of the land sparing modelling and estimation of attainable yields are addressed in Supplementary Text S4.

### **Definition of biodiversity hotspots**

Biodiversity hotspots were defined based on rarity-weighted richness as the sum of number of species present in a grid cell weighted by their range size (1/Area of Habitat (AOH))<sup>65</sup>. Higher values occur in grid cells rich in species with small ranges. These cells have a large global responsibility for species conservation. Rarity-weighted richness was quantified in absolute terms and in addition normalized per WWF ecoregion<sup>66</sup> and continent to account for regions of (a) high absolute importance for biodiversity, which are typically concentrated in the tropics, and (b) regional importance for biodiversity within specific ecoregions<sup>44</sup>. From both resulting datasets, the 90<sup>th</sup> percentile was selected to be abandoned for targeted land sparing in the TLS scenario (Supplementary Figure S16).

### **Quantification of agricultural externalities**

#### *Crop nutrient requirements*

N, P, and irrigation water were applied by the EPIC model based on deficits compared with optimal supply and relative crop stress thresholds (see Supplementary Methods S2). The model considered losses (leaching, runoff, erosion, immobilization, and gaseous emissions) and limited the number of crop management operations to a level common to current management practices (annual application of P, and restricted number of applications for N and water within a given time period) to represent an optimal management strategy that balances realistic overheads for plant nutrient inputs. Fertilizer requirements for crops that were not considered in the optimization were derived from the proportions of crop-specific fertilizer application rates around 2000<sup>19</sup> to total fertilizer application volumes during the 2011-2015 reference period, as reported in FAOSTAT<sup>29</sup>.

Besides exogenous inputs, nutrients used by crop plants are also sourced from soil stocks and mineralization of organic matter as well in the field as in the crop model. While these represent a substantial short-term source of nutrients, depletion occurs over time that may lead to the underestimation of fertilizer requirement. Amounts of N and P required for sustainable nutrient replenishment in such cases were estimated from a fertilizer requirement of 120% of crop uptake. For soils with high or very high P immobilization potential<sup>67</sup>, we ensured the fertilizer requirement was twice the crop uptake<sup>38</sup>. For leguminous crops (groundnuts, pulses, and soybean), we assumed that at yields >2.5 t ha<sup>-1</sup>, only 80% of N demand is met through fixation<sup>68</sup>, and added 20% of crop uptake as supplementary fertilizer. More details on the *ex-post* accounting for potentially higher nutrient requirements than estimated by the crop model are provided in Supplementary Methods S3.

#### *Nutrients in plant residues and manure*

N and P embodied in removed crop residues (straw, stalks, stover) or burning of crop residues in the field were not modelled explicitly. To account for removal of N and P from the field as post-harvest residues in supplementary evaluations, we estimated crop residue dry matter from reference period

crop production volumes<sup>23</sup> and crop harvest indices in the EPIC model, and then calculated volumes of N and P based on the USDA crop nutrient tool<sup>69</sup>. National crop-specific residue removal and burning rates were obtained from a recent global report<sup>70</sup> that covers all crops included in this study, with the exception of sugar beet, groundnut, pulses, millet, and rice. For the first four of these crops, we approximated values using coefficients of potato for sugar beet, soybean for groundnuts and pulses, and sorghum for millet. For countries lacking data, we applied a mean based on major UN regions. Data for rice were obtained from a recent literature review<sup>4</sup>. For burned residue, we assumed that 80% of N and 40% of P are lost as emissions. Total removal from the field amounted to 19.6 Tg N and 2.2 Tg P, respectively. Fertilizer requirements were scaled according to a fertilizer:uptake ratio in crop yield, to account for additional losses due to increased fertilizer application. Present amounts of N and P contributed by manure cycling to cropland were estimated from the literature as 17.3 Tg and 4.2 Tg, respectively<sup>71,72</sup>. The additional or reduced requirements for N and P replenishment with present rates of residue removal and manure application, as well as uncertainties in the nutrient budgets, are discussed in Supplementary Text S3.

#### Irrigation water requirement

Irrigation water requirements estimated by the EPIC model to meet plant water demand do not consider inefficiencies due to losses during the extraction to field application process. These may be more than twice the actual plant demand, depending on the irrigation system in place<sup>41</sup>. For the relative change in irrigation water requirement for the crops considered, we compare the irrigation requirement on the total cropland to that in each land sparing scenario. To account for the crops not considered in the simulations, we scaled crop-specific irrigation water requirements from a study based on the Global Crop Water Model (GCWM) model that considers all major crops or crop groups<sup>3</sup>.

Expansion of irrigated land would also provide a means for increasing crop yields<sup>73</sup> and accordingly decreasing land requirement. We do not consider this option here due to its lower flexibility compared to nutrient input intensification as (a) it requires upfront investment in infrastructure, (b) it is subject to policy and governance decisions on water resources, (c) it is subject to competition among sectors, and (d) inter-annual variations in water availability for irrigation affect crops differently *in-situ* based on economic considerations among others<sup>74</sup>.

#### Greenhouse gas emissions

Greenhouse gas emissions in CO<sub>2</sub> equivalents were calculated following the tier 1 methodology of FAO<sup>75</sup> for the major cropland emission contributors of paddy rice fields (CH<sub>4</sub>) and nitrogen fertilizer (N<sub>2</sub>O), based on fixed N<sub>2</sub>O emissions per unit of applied fertilizer and national coefficients of CH<sub>4</sub> emissions ha<sup>-1</sup> of harvested paddy rice. Other emissions, for example from manure and crop residues, were assumed to remain constant. Estimates of emissions of N<sub>2</sub>O for crops not considered in the optimization were based on N fertilizer requirements, as calculated above.

#### Carbon in potential natural vegetation

The potential loss of C from natural vegetation expected to develop on spared cropland has been investigated by West et al.<sup>39</sup> to quantify C losses in food production. Using the publically available dataset of C stored in potential natural vegetation [t ha<sup>-1</sup>], we quantified reductions in C loss following minimization of cropland area compared with the baseline cropland area in the SPAM 2005 v3.2

database for crops considered in the optimization and for other crops, separately. The exact calculation is provided in Supplementary Methods S4.

#### Area of habitat

We modeled the Area of Habitat (AOH) for each terrestrial mammal species with range data and habitat preferences available from the IUCN Red List database (accessed April 2018). The AOH is defined as the area characterized by abiotic and biotic properties that is habitable by a particular species. Specifically, we modelled the AOH as the areas that (i) fall within the mapped range and (ii) map to the known habitat preferences of the species. The species ranges of terrestrial mammals were downloaded from the IUCN database. We considered only habitat types coded as ‘suitable’ by taxonomic experts within the IUCN database. In absence of a map of IUCN habitat classes, and similarly to all previous work modelling of AOH<sup>44,45</sup>, we cross-walked the IUCN habitat classes into an existing land-use product to translate habitat preferences into land-cover and land-use preferences. Accordingly, our assessment only accounts for biogeographic distributions of species habitats but not for impacts of land use intensification on wild species on cropland *in situ*.

As land-cover base layer we used the European Space Agency CCI (ESA-CCI) land-cover map for the year 2015<sup>76</sup> and re-allocated cropland areas as calculated from the SPAM2005 baseline or the land sparing scenarios, including annual and perennial crops not considered in the land use model to account for all cropland. When cropland area was higher than estimated in the ESA-CCI map, the additional area was allocated to all natural land-cover types (except water and ice) in proportion to their extent in the grid cell. Similarly, when cropland area was lower than estimated in the ESA-CCI map, the excess cropland was allocated to all natural land-cover types (except water and ice) in proportion to their extent in the grid cell. We then summarized the results as distribution of AOH changes in optimized versus baseline scenarios across all species, species sensitive to cropland areas (those for which cropland is considered unsuitable according to IUCN habitat preferences), species in the lower quartile of range-size distribution, and species in the lower quartile of range-size distribution sensitive to cropland areas. The latter was selected as the main results, outcomes for the other species sub-selections are presented in Supplementary Figure S17.

#### **Data processing and visualization**

Evaluations were performed in R<sup>77</sup>, and plots were produced using ggplot2<sup>78</sup> and rasterVis<sup>79</sup>. The visualization of simulation units in Supplementary Figure S19 was produced with ESRI ArcGIS 10.7.

**Correspondence and requests for materials** should be addressed to CF

#### **Acknowledgements**

CF, NK, JB, RS, PC, IAJ, JP, and MO were supported by European Research Council Synergy grant ERC-2013-SynG-610028 Imbalance-P. We gratefully acknowledge the provision of threatened species data by IUCN and the provision of land cover data by the ESA CCI Land Cover project.

#### **Author contributions**



524 CF, NK, and MO designed the study; CF and NK performed central analyses; JB, RS, and PV contributed  
525 models and data; CF wrote an initial draft; all authors contributed substantially to interpretation of the  
526 results and revisions of the manuscript.

527 **Data availability**

528 The datasets generated during the current study are available from an FTP server for review purposes:  
529 [http://user.iiasa.ac.at/~folberth/land\\_sparing/](http://user.iiasa.ac.at/~folberth/land_sparing/). They will be made available in a public repository upon  
530 publication.

531

## References (including Methods)

1. van der Velde, M. *et al.* African crop yield reductions due to increasingly unbalanced Nitrogen and Phosphorus consumption. *Global Change Biology* **20**, 1278–1288 (2014).
2. MacDonald, G. K., Bennett, E. M., Potter, P. A. & Ramankutty, N. Agronomic phosphorus imbalances across the world's croplands. *Proceedings of the National Academy of Sciences* **108**, 3086–3091 (2011).
3. Siebert, S. & Döll, P. Quantifying blue and green virtual water contents in global crop production as well as potential production losses without irrigation. *Journal of Hydrology* **384**, 198–217 (2010).
4. Carlson, K. M. *et al.* Greenhouse gas emissions intensity of global croplands. *Nature Climate Change* **7**, 63–68 (2017).
5. Steffen, W. *et al.* Planetary boundaries: Guiding human development on a changing planet. *Science* **347**, 1259855 (2015).
6. Balmford, A. & Green, R. How to spare half a planet. *Nature* <http://www.nature.com/articles/d41586-017-08579-6> (2017) doi:10.1038/d41586-017-08579-6.
7. Ewers, R. M., Scharlemann, J. P. W., Balmford, A. & Green, R. E. Do increases in agricultural yield spare land for nature? *Global Change Biology* **15**, 1716–1726 (2009).
8. Phalan, B. *et al.* How can higher-yield farming help to spare nature? *Science* **351**, 450–451 (2016).
9. Salles, J.-M., Teillard, F., Tichit, M. & Zanella, M. Land sparing versus land sharing: an economist's perspective. *Reg Environ Change* **17**, 1455–1465 (2017).
10. Wilson, E. O. *Half-earth: our planet's fight for life*. (WW Norton & Company, 2016).

- 555 11. Bodirsky, B. L. *et al.* Global Food Demand Scenarios for the 21st Century. *PLOS ONE*  
556 **10**, e0139201 (2015).
- 557 12. Popp, A. *et al.* Land-use futures in the shared socio-economic pathways. *Global*  
558 *Environmental Change* **42**, 331–345 (2017).
- 559 13. Nelson, G. C. *et al.* Climate change effects on agriculture: Economic responses to  
560 biophysical shocks. *PNAS* **111**, 3274–3279 (2014).
- 561 14. Mehrabi, Z., Ellis, E. C. & Ramankutty, N. The challenge of feeding the world while  
562 conserving half the planet. *Nature Sustainability* **1**, 409–412 (2018).
- 563 15. Erb, K.-H. *et al.* Exploring the biophysical option space for feeding the world without  
564 deforestation. *Nature Communications* **7**, 11382 (2016).
- 565 16. Springmann, M. *et al.* Options for keeping the food system within environmental limits.  
566 *Nature* **562**, 519–525 (2018).
- 567 17. Balkovič, J. *et al.* Global wheat production potentials and management flexibility under  
568 the representative concentration pathways. *Global and Planetary Change* **122**, 107–121  
569 (2014).
- 570 18. Mauser, W. *et al.* Global biomass production potentials exceed expected future demand  
571 without the need for cropland expansion. *Nature Communications* **6**, 8946 (2015).
- 572 19. Mueller, N. D. *et al.* Closing yield gaps through nutrient and water management. *Nature*  
573 **490**, 254–257 (2012).
- 574 20. Koh, L. P., Koellner, T. & Ghazoul, J. Transformative optimisation of agricultural land  
575 use to meet future food demands. *PeerJ* **1**, e188 (2013).

- 576 21. Davis, K. F., Rulli, M. C., Seveso, A. & D’Odorico, P. Increased food production and  
577 reduced water use through optimized crop distribution. *Nature Geoscience* **10**, 919–924  
578 (2017).
- 579 22. Balmford, A., Green, R. & Phalan, B. Land for Food & Land for Nature? *Daedalus* **144**,  
580 57–75 (2015).
- 581 23. Balmford, A. *et al.* The environmental costs and benefits of high-yield farming. *Nature*  
582 *Sustainability* **1**, 477–485 (2018).
- 583 24. Ray, D. K., Ramankutty, N., Mueller, N. D., West, P. C. & Foley, J. A. Recent patterns of  
584 crop yield growth and stagnation. *Nature Communications* **3**, 1293 (2012).
- 585 25. Williams, J. R. The erosion-productivity impact calculator (EPIC) model: a case history.  
586 *Phil. Trans. R. Soc. Lond. B* **329**, 421–428 (1990).
- 587 26. Izaurrealde, R. C., Williams, J. R., McGill, W. B., Rosenberg, N. J. & Jakas, M. C. Q.  
588 Simulating soil C dynamics with EPIC: Model description and testing against long-term data.  
589 *Ecological Modelling* **192**, 362–384 (2006).
- 590 27. Feniuk, C., Balmford, A. & Green, R. E. Land sparing to make space for species  
591 dependent on natural habitats and high nature value farmland. *Proceedings of the Royal*  
592 *Society B: Biological Sciences* **286**, 20191483 (2019).
- 593 28. Schulte, L. A. *et al.* Prairie strips improve biodiversity and the delivery of multiple  
594 ecosystem services from corn–soybean croplands. *PNAS* **114**, 11247 (2017).
- 595 29. FAO. *FAOSTAT statistical database*. (2016).
- 596 30. Schleicher, J. *et al.* Protecting half of the planet could directly affect over one billion  
597 people. *Nat Sustain* (2019) doi:10.1038/s41893-019-0423-y.
- 598 31. Ellis, E. C. Sharing the land between nature and people. *Science* **364**, 1226–1228 (2019).

- 599 32. Verburg, P. H., Mertz, O., Erb, K.-H., Haberl, H. & Wu, W. Land system change and  
600 food security: towards multi-scale land system solutions. *Current Opinion in Environmental*  
601 *Sustainability* **5**, 494–502 (2013).
- 602 33. Puma, M. J., Bose, S., Chon, S. Y. & Cook, B. I. Assessing the evolving fragility of the  
603 global food system. *Environ. Res. Lett.* **10**, 024007 (2015).
- 604 34. Alston, J. M., Babcock, B. A. & Pardey, P. G. *The shifting patterns of agricultural*  
605 *production and productivity worldwide*. (Midwest Agribusiness Trade Research and  
606 Information Center, 2010).
- 607 35. Müller, D. *et al.* Regime shifts limit the predictability of land-system change. *Global*  
608 *Environmental Change* **28**, 75–83 (2014).
- 609 36. Kastner, T., Erb, K.-H. & Haberl, H. Rapid growth in agricultural trade: effects on global  
610 area efficiency and the role of management. *Environ. Res. Lett.* **9**, 034015 (2014).
- 611 37. Barzman, M. *et al.* Eight principles of integrated pest management. *Agron. Sustain. Dev.*  
612 **35**, 1199–1215 (2015).
- 613 38. Roy, E. D. *et al.* The phosphorus cost of agricultural intensification in the tropics. *Nature*  
614 *Plants* **2**, 16043 (2016).
- 615 39. West, P. C. *et al.* Trading carbon for food: Global comparison of carbon stocks vs. crop  
616 yields on agricultural land. *Proceedings of the National Academy of Sciences* **107**, 19645–  
617 19648 (2010).
- 618 40. IUCN. The IUCN Red List of Threatened Species. <https://www.iucnredlist.org>. (2018).
- 619 41. Jägermeyr, J. *et al.* Water savings potentials of irrigation systems: global simulation of  
620 processes and linkages. *Hydrol. Earth Syst. Sci.* **19**, 3073–3091 (2015).

- 621 42. Sterling, S. M., Ducharne, A. & Polcher, J. The impact of global land-cover change on  
622 the terrestrial water cycle. *Nature Climate Change* **3**, 385–390 (2013).
- 623 43. Folberth, C., Yang, H., Gaiser, T., Abbaspour, K. C. & Schulin, R. Modeling maize yield  
624 responses to improvement in nutrient, water and cultivar inputs in sub-Saharan Africa.  
625 *Agricultural Systems* **119**, 22–34 (2013).
- 626 44. Leclere, D. *et al.* Towards pathways bending the curve of terrestrial biodiversity trends  
627 within the 21st century. <http://pure.iiasa.ac.at/id/eprint/15241/> (2018).
- 628 45. Visconti, P. *et al.* Projecting Global Biodiversity Indicators under Future Development  
629 Scenarios. *Conservation Letters* **9**, 5–13 (2016).
- 630 46. Phalan, B. T. What Have We Learned from the Land Sparing-sharing Model?  
631 *Sustainability* **10**, 1760 (2018).
- 632 47. Tscharntke, T., Klein, A. M., Kruess, A., Steffan Dewenter, I. & Thies, C. Landscape  
633 perspectives on agricultural intensification and biodiversity – ecosystem service management.  
634 *Ecology Letters* **8**, 857–874 (2005).
- 635 48. Stehfest, E. *et al.* Key determinants of global land-use projections. *Nature*  
636 *Communications* **10**, 2166 (2019).
- 637 49. Schmitz, C. *et al.* Land-use change trajectories up to 2050: insights from a global agro-  
638 economic model comparison. *Agricultural Economics* **45**, 69–84 (2014).
- 639 50. Schmidt-Traub, G., Obersteiner, M. & Mosnier, A. Fix the broken food system in three  
640 steps. *Nature* **569**, 181–183 (2019).
- 641 51. Müller, C., Bondeau, A., Lotze Campen, H., Cramer, W. & Lucht, W. Comparative  
642 impact of climatic and nonclimatic factors on global terrestrial carbon and water cycles.  
643 *Global Biogeochemical Cycles* **20**, (2006).

52. Müller, C. *et al.* Global gridded crop model evaluation: benchmarking, skills, deficiencies and implications. *Geosci. Model Dev.* **10**, 1403–1422 (2017).
53. Balkovič, J. *et al.* Impacts and Uncertainties of +2°C of Climate Change and Soil Degradation on European Crop Calorie Supply. *Earth's Future* **6**, 373–395 (2018).
54. Balkovič, J. *et al.* Pan-European crop modelling with EPIC: Implementation, up-scaling and regional crop yield validation. *Agricultural Systems* **120**, 61–75 (2013).
55. Folberth, C. *et al.* Uncertainty in soil data can outweigh climate impact signals in global crop yield simulations. *Nature Communications* **7**, 11872 (2016).
56. FAO, IIASA, ISRIC, ISSCAS & JRC. Harmonized World Soil Database (version 1.2). (2012).
57. US Geological Survey. GTOPO30 - 30 arc seconds digital elevation model from US Geological Survey. (2002) doi:<https://doi.org/10.5066/F7DF6PQS>.
58. Skalský, R. *et al.* GEO-BENE global database for bio-physical modeling. *GEOBENE project* (2008).
59. Ruane, A. C., Goldberg, R. & Chryssanthacopoulos, J. Climate forcing datasets for agricultural modeling: Merged products for gap-filling and historical climate series estimation. *Agricultural and Forest Meteorology* **200**, 233–248 (2015).
60. Sacks, W. J., Deryng, D., Foley, J. A. & Ramankutty, N. Crop planting dates: an analysis of global patterns. *Global Ecology and Biogeography* **19**, 607–620 (2010).
61. You, L., Wood, S., Wood-Sichra, U. & Wu, W. Generating global crop distribution maps: From census to grid. *Agricultural Systems* **127**, 53–60 (2014).
62. Porwollik, V. *et al.* Spatial and temporal uncertainty of crop yield aggregations. *European Journal of Agronomy* **88**, 10–21 (2017).

- 667 63. Portmann, F. T., Siebert, S. & Döll, P. MIRCA2000—Global monthly irrigated and  
668 rainfed crop areas around the year 2000: A new high-resolution data set for agricultural and  
669 hydrological modeling. *Global Biogeochemical Cycles* **24**, (2010).
- 670 64. Monfreda, C., Ramankutty, N. & Foley, J. A. Farming the planet: 2. Geographic  
671 distribution of crop areas, yields, physiological types, and net primary production in the year  
672 2000. *Global Biogeochemical Cycles* **22**, 1–19 (2008).
- 673 65. Albuquerque, F. S. de & Gregory, A. The geography of hotspots of rarity-weighted  
674 richness of birds and their coverage by Natura 2000. *PLOS ONE* **12**, e0174179 (2017).
- 675 66. Olson, D. M. *et al.* Terrestrial Ecoregions of the World: A New Map of Life on Earth.  
676 *BioScience* **51**, 933–938 (2001).
- 677 67. Batjes, N. H. *Global distribution of soil phosphorus retention potential*. (2011).
- 678 68. Cafaro La Menza, N., Monzon, J. P., Specht, J. E. & Grassini, P. Is soybean yield limited  
679 by nitrogen supply? *Field Crops Research* **213**, 204–212 (2017).
- 680 69. Crop Nutrient Tool | USDA PLANTS. <https://plants.usda.gov/npk/main>.
- 681 70. R Köble. The global nitrous oxide calculator – GNOC – Online tool manual v1.2.4.  
682 (2014).
- 683 71. Liu, J. *et al.* A high-resolution assessment on global nitrogen flows in cropland.  
684 *Proceedings of the National Academy of Sciences* **107**, 8035–8040 (2010).
- 685 72. Bouwman, L. *et al.* Exploring global changes in nitrogen and phosphorus cycles in  
686 agriculture induced by livestock production over the 1900–2050 period. *Proc Natl Acad Sci*  
687 *USA* **110**, 20882 (2013).
- 688 73. Jägermeyr, J. *et al.* Integrated crop water management might sustainably halve the global  
689 food gap. *Environ. Res. Lett.* **11**, 025002 (2016).



690 74. Qin, Y. *et al.* Flexibility and intensity of global water use. *Nat Sustain* **2**, 515–523 (2019).

691 75. Tubiello, F. N. *et al.* The FAOSTAT database of greenhouse gas emissions from

692 agriculture. *Environmental Research Letters* **8**, 015009 (2013).

693 76. Bontemps, S. *et al.* Consistent global land cover maps for climate modelling

694 communities: current achievements of the ESA’s land cover CCI. in *Proceedings of the ESA*

695 *Living Planet Symposium, Edinburgh* 9–13 (2013).

696 77. RDevelopment Core Team. *R: A language and environment for statistical computing*. (R

697 foundation for statistical computing Vienna, Austria, 2008).

698 78. Wickham, H. *ggplot2: elegant graphics for data analysis*. (Springer, 2016).

699 79. Perpinan, O. & Hijmans, R. rasterVis. *R package version 0.41* (2016).

700